



CHALMERS
UNIVERSITY OF TECHNOLOGY

Joint Design and Co-integration of Antenna-IC Systems

Downloaded from: <https://research.chalmers.se>, 2026-04-04 19:21 UTC

Citation for the original published paper (version of record):

Ivashina, M. (2019). Joint Design and Co-integration of Antenna-IC Systems. 13th European Conference on Antennas and Propagation, EuCAP 2019

N.B. When citing this work, cite the original published paper.

Joint Design and Co-integration of Antenna-IC Systems

Marianna. V. Ivashina¹,

¹Chalmers, Department of Electrical Engineering, Göteborg, Sweden, marianna.ivashina@chalmers.se

Abstract—An overview of design challenges for beamforming active antenna arrays, which are needed to meet high-performance demands of future emerging applications, is presented. The critical role of antenna element mutual coupling on the receiving system sensitivity of array receivers, and effective radiated power of MIMO-type array transmitters is discussed. Trade-offs, common misconceptions, and practical examples are shown and discussed. Techniques towards strong integration between antennas and LNAs/PAs that blurs the geometrical boundaries between them are presented. This will cover mm-wave antenna design examples, where direct matching of active devices to their optimal source/load impedances eliminates the losses of 50-Ohm impedance matching networks. An antenna-integrated high-efficiency (Doherty) PA, operating at the sub-6 GHz band and utilizing active load modulation, will be taken as an on-antenna power combining example, including optimization aspects and over-the-air characterization.

Index Terms—Co-design, co-integration, antennas, amplifiers

I. INTRODUCTION

Conventionally, the microwave and antenna research fields have developed as separate disciplines, using distinct modeling methodologies and relying on good isolation between individually optimized system components. However, the past decade has seen a dramatic departure from classical methodologies towards system-level optimal designs, as needed to meet high-performance demands of future emerging applications (e.g., 5G and future connectivity, autonomous driving, Space exploration).

Antenna systems for such applications typically involve arrays of many antenna elements and active front ends, with power amplifiers (PAs) and low noise amplifiers (LNAs) in the proximity to the antenna or even integrated with the antenna. Such systems require a combined circuit-electromagnetic modeling approach, and these are nonreciprocal and potentially nonlinear. Furthermore, array beamforming and signal processing should be considered from the start to enable full system analysis and design optimization. A key result of the past decades of research in this area is the understanding that antenna element mutual coupling has a significant impact on the overall system performance, and requires important trade-offs to be made in the design process. On the one hand, strong antenna mutual coupling effects can be used to enhance the beam scanning range and frequency bandwidth in terms of the antenna impedance and efficiency [1]. On the other hand, these effects result in a strong correlation between the signal & noise waves propagating through the system, and hence strong noise coupling effects between LNAs (and lower SNR) of receiving

systems, or strong non-linear distortion effects between PAs (and lower effective radiated power) of transmitting systems occur [2], [3].

In this paper, a modern approach to the design of active beamforming array antennas in the receiving situation that reflects the state-of-the-art in the academic literature is presented. This approach has been included in the recently published textbook [2]. Techniques for the optimal noise match of a multi-channel receiver to an array antenna, in the presence of antenna mutual coupling effects and associated noise coupling phenomena, are discussed — including trade-offs, common misconceptions, and practical examples.

Afterwards, the latest studies highlighting some of the current research involving circuit-antenna co-integration solutions for active beamforming transmitting array antennas are presented. The focus is on integration strategies which are tailored to high-efficiency PA architectures and suited for applications with demanding performance requirements. An antenna-integrated high-efficiency (Doherty) PA utilizing active load modulation will be taken as an on-antenna power combining example, including optimization aspects and over-the-air characterization methods. Other examples will cover novel mm-wave circuit-antenna transitions employing a direct antenna-PA impedance matching technique.

II. BEAMFORMING ARRAY RECEIVERS

A. Application requirements

High-sensitive receiving array antennas find application in radio astronomy, satellite communications, active and passive remote sensing, and other microwave sensing areas [2], [4]–[11]. The common denominator of these applications is that the external microwave sky noise environment as seen by the receiver has a low brightness temperature, which is only a couple of Kelvin at L-band. As a consequence, the incremental improvements of receiver noise figure and antenna radiation efficiency are much more critical than for terrestrial communication and radar applications, for which the external noise contribution is typically dominated by interference from other transmitters. As detailed later in this section, a significant research effort has been made towards the increased level of integration between the receiving antenna elements and LNAs in order to minimize the self-generated system noise contributions, i.e. due to Ohmic losses in the array elements, and receiver noise introduced by LNAs and electronics in the signal paths after the antenna elements.

TABLE I
COMPARISON OF APPLICATIONS FOR ARRAY RECEIVERS AND TRANSMITTERS

Specific conditions and requirements	Receivers			Transmitters		
	Radio astronomy	Passive remote sensing	Satellite communication	Defense	Space-borne communications	Terrestrial cellular communications
Location of antenna	ground	space	space/ground, cars, airplanes	fixed or mobile platform	space	walls, masts
Strength and origin of signals of interest	weak, distant natural emissions	weak, distant natural emissions	strong, distant man-made signals	strong, distant man-made signals	strong, distant man-made signals	strong at sub-6GHz bands, weaker at mm-wave bands
RFI situation	RFI quiet area	rich RFI	minor importance	RFI eavesdropping/jamming	minor importance	important from other transmitters
Key performance metrics	A_e/T_{sys} , ant. efficiency, system noise temp.	radiometric res., bias, spatial res.	G/T_{sys} , polarization purity, min. adjacent satellite interference, scan range, cost	footprint and volume coverage, power efficiency, cost in relative terms	coverage, beamwidth, power efficiency, robustness to manufact. and operational tolerances	coverage, capacity, user throughput, power efficiency, footprint, ease of deployment, cost
Physical size of the array aperture	AA: 1 to 100 m ² , PAF: 1 × 1 m ²	~1-1.5 meter	Typically ~1 meter or smaller	for small integrated arrays, 100 mm diameter, 50 mm depth	depends on coverage and number of beams	128 or more elements, potentially 500-1000
Bandwidth	(ultra-)wide	multi-band, narrow	50-500 MHz	6-18, 26-40 GHz, 1-20% depend. on coverage	17.5-20.2 GHz, 10-15%	sub-6GHz (10% and more), 12-30 GHz (10%)
Output power per element (peak)	–	–	–	0.1 Watt	1 Watt CW (≤ 20 GHz), 0.1 Watt CW (≤ 40 GHz)	15-20 dBm
Sidelobe levels	low-moderate	very low	critical for uplink, less for downlink	low-moderate	critical for uplink, less for downlink	less critical
Cross-polarization level/purity	low-moderate	very low	very low	low-moderate	very low	low-moderate

While maximizing the Signal-To-Noise Ratio (SNR) and receiving sensitivity it is of paramount importance to weigh in other performance metrics, such as beam shape, sidelobe levels, and polarization purity, depending on the particular operating conditions of the antenna and application specific requirements (cf. Table I). To achieve the desired performance, modern array antenna systems use digital signal processing and beamforming algorithms to control the phases and amplitudes of the antenna element weights.

B. Design challenges

An important lesson of the last decade research in the area of high-sensitivity receiving array antennas is that of maximizing the receiver SNR. LNAs must be noise-matched to active reflection coefficients (scan impedances) of the array antenna elements, rather than passive reflection coefficients (passive impedances) as traditionally done [12], [13]. Furthermore, since all elements may have different weights when they are used to form certain optimum beam characteristics, and because each element may contribute simultaneously to several beams (a typical situation for digital beamforming arrays), the array element excitation environment varies. This implies that all noise temperature contributions (e.g. due to antenna losses and noisy LNAs) are dependent on the beamformer weights and hence also vary with the beam scan angle. The variation in the system noise temperature within the required scan-angle range that is caused solely by a change in the noise coupling

contribution can be as large as 30% [14], this is in the order of 10-15 Kelvin for L-band room-temperature aperture array (AA) receivers.

To account for these important relations between antenna element mutual coupling, array receiver noise, and beamformer weights, various complementary methods have been developed, including: (i) numerical methods for characterizing a complete (final) system that includes an antenna array, multi-channel receiver, and beamforming network [15]–[19]; and (ii) practical figures of merit [20]–[22] and measurement procedures [14] based on analytic methods which tie together network, antenna analysis, and microwave noise theories. The latter methods allow predominant factors affecting the overall system performance to be isolated and analyzed in detail, and thus are useful for design optimization. Examples of such figures of merit are the sub-efficiencies and system noise temperature of a receiving antenna array that can be expressed analytically in terms of the isotropic noise response of the array [20] or through an equivalent system representation [21], [22].

Another important result from the above research work is the proposed new terms for active antenna arrays [23], which have been included in the most recent revision of the *IEEE Standard for Definitions of Terms for Antennas* [24]. The terms which have been added or updated are isotropic noise response, active antenna available gain, active antenna

available power, receiving efficiency, effective area for active arrays, noise matching efficiency, and noise temperature for active arrays.

C. Integration methods

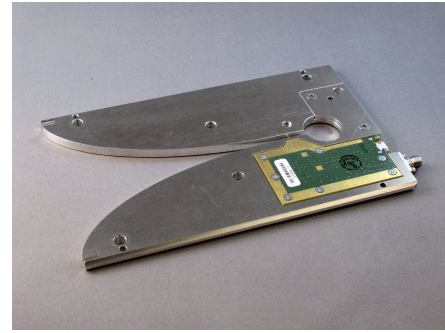
To improve the receiving sensitivity, various integration approaches have been implemented. A common starting point is to select an element type according to the operating frequency and bandwidth, and optimize its geometry numerically to achieve an optimal active impedance noise match to a given LNA, as well as high aperture efficiency so that the overall system sensitivity is maximized [25], [26]. For large-scale arrays, this is often done using infinite array simulations as the initial starting point, where the objective is to minimize the variation of the active impedance that satisfies the optimal noise-match condition over the operating frequency bandwidth and scan range [19], [27].

The above integration approach can be extended by matching the antenna element to the optimal noise impedance of the LNA, without extra impedance matching network on the antenna structure, so as to maximize the antenna radiation efficiency and reduce the system noise temperature [28], [29]. As an example, the ambient-temperature array LNAs in [28] have been designed specifically for the phased-array feed (PAF) applications in radio telescopes with the particular focus on the minimum array noise performance (see Fig. 1), and have shown to yield the array beam-equivalent noise temperatures as low as 20 Kelvin. This is over 10 Kelvin improvement in the receiver noise temperature, and is the state of the art in terms of array beam-equivalent noise temperatures at these frequencies. Further improvement in the system performance can be achieved by avoiding any intermediate feeding lines and impedance matching networks between the antenna element and LNA; one complication is, however, to maintain a desired wide bandwidth and large scan range for such implementations.

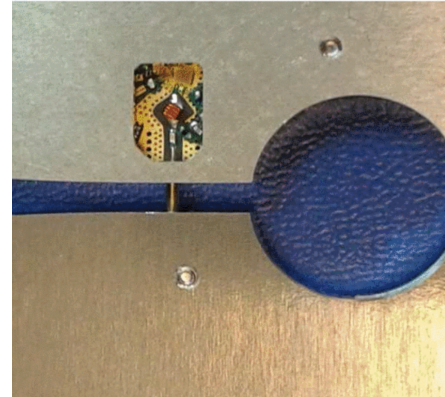
III. BEAMFORMING ARRAY TRANSMITTERS

A. Application requirements

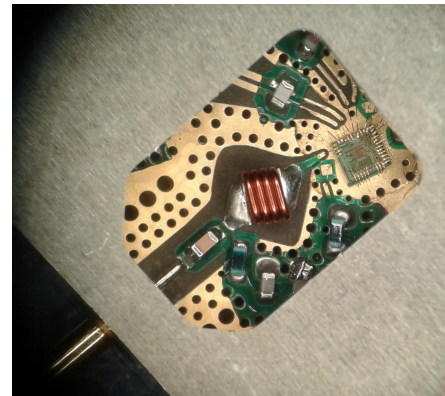
The continued growth in data traffic, both in terrestrial wireless and space-based communications, implies that conventional antenna technologies presently in use will not suffice in supporting future demands. Instead, array antenna systems with a large number of active antenna elements and advanced beamforming capabilities, such as massive MIMO (Multiple-Input and Multiple-Output) arrays [30], are required. However, the implementation of such complex systems into energy- and cost-effective solutions has been proven very challenging, due to the combination of multiple demanding performance characteristics, and application specific constraints. Table I provides a brief overview of emerging use-cases of integrated transmitting arrays for three application domains, i.e. space-based communication, defense-oriented applications, and terrestrial cellular wireless communications [31], [32]. As can be seen, a common design goal for such systems is high effective radiated power with minimum size, weight, and cost.



(a)



(b)



(c)

Fig. 1. LNA-integrated Tapered Slot Antenna (TSA) element of a phased array receiver operating at 0.7–1.5 GHz: (a) Antenna element with the 65-nm CMOS LNA (seen on the underside of the green printed-circuit board) where coupling from the slotline to the LNA is realized by a pin, which is visible in (b-c) that extends across the slot and is terminated in a grounded socket. ©2016, IEEE. Reprinted, with permission, from [28, Fig. 1 and Fig. 2].

B. Design challenges

One important lesson of the research in this area is that power amplifiers (PAs) should be directly matched to their optimal load and source impedances for maximize output power and efficiency, while eliminating 50-Ohm reference impedance and matching networks that may increase losses, size, and cost as well as reduce the bandwidth the larger the impedance transformation is [33], [34]. For practical PAs and radiating antenna elements, this can be challenging as the optimal load impedance values for practical PAs and antennas

are profoundly distinct. A PA prefers a relatively small load resistance, which is typically related to the breakdown voltage of the semiconductor technology (e.g. 4-5 Ohm for CMOS and 17-20 Ohm for GaN HEMT at 20GHz), and relatively large inductive load. At the same time, conventional antenna designs prefer relatively high resistance values, which are more close to 50-Ohm for higher radiation efficiency. Therefore, direct optimal antenna-PA matching requires a trade-off between the antenna radiation efficiency (which are affected by the antenna dimensions), and the optimal PA load impedance on the other hand [32], [35]. It is worth mentioning, however, that this trade-off does not apply to general antenna classes and is mainly relevant to electrically small antennas. In [32], it has been shown that an electrically small loop antenna (with the circumference of 0.25 wavelength), which is directly matched to the PA optimal load impedance, has the radiation efficiency of approximately 26%, while the PA power added efficiency (PAE) is 15%. The efficiency values can be improved by increasing the antenna dimensions that would also lead to a deterioration of the PAE to be lower than 15%, and vice versa.

Furthermore, circuit losses associated with power combining can be avoided by utilizing the antenna itself for power combining [33], [36]–[38]. This can also help to reduce the heat dissipation problems utilizing the metal parts of the antenna as the heat sink, and yields a more compact design [35]. These important findings have motivated new non-conventional design concepts, where an antenna can provide multiple functionalities, i.e. radiation, PA-impedance-matching, PA-tailored-power-combining, filtering, etc. Examples are the integration concepts involving antenna elements with distributed multi-point feeding or contactless EM-coupling based transitions to multiple PAs [38]–[41].

The concepts in [35], [40], [41] (see Figs. 2, 3, and 4) will be discussed during the presentation, and be used to highlight the current trends in mm-wave antenna design towards more generalized forms of integration, where the geometrical boundaries between individual components (e.g. antennas, PAs) are blurred, and the antenna and PAs are merged into a single medium [42]–[44].

C. Integration methods

A literature survey on this subject shows that the above integration techniques have been demonstrated primarily for single antenna elements and conventional relatively inefficient (e.g. single-ended class-B) PA architectures, where the focus was on improved performance at peak power levels [39], [45]–[47]. Significantly fewer publications are dedicated to integrated antenna-PA systems that can enable much higher efficiency at backed-off power levels where the probability density of communication signals is highest [48]–[50].

Recently, novel design methods using antenna-integrated Doherty power amplifiers (DPAs) have been proposed to increase efficiency at back-off power levels [52]–[54]. The DPA architectures are based on active load modulation between a main- and an auxiliary PA that is traditionally realized by a tailored circuit combiner network before the antenna. However,

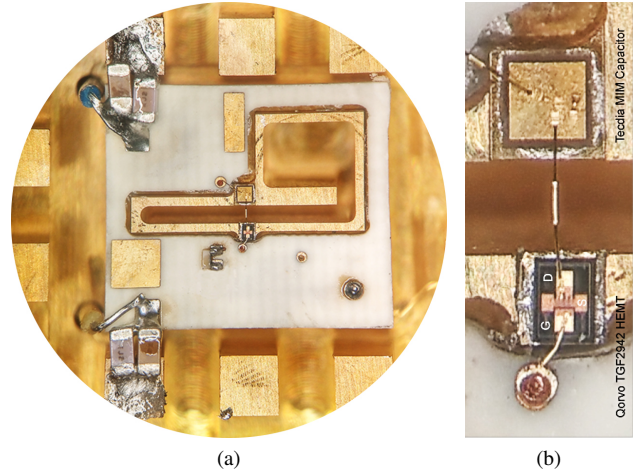


Fig. 2. Antenna integration approach employing direct impedance matching to the PA, without intermediate impedance matching circuitry: (a) A K-band PA-Integrated active b-shaped slot antenna on a ground plane comprising a bed of nails (dimensions: 9.1mm×7.3mm) [35]. (b) The drain of the Qorvo GaN HEMT die is directly integrated over the radiating slot and bonded to the Teccia MIM (Metal-Insulator-Metal) capacitor.

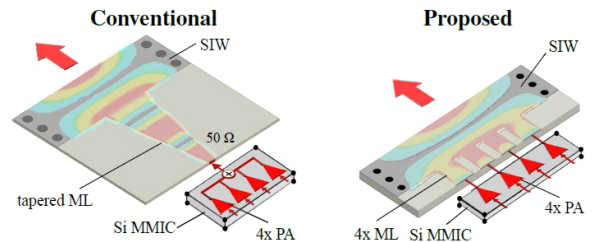


Fig. 3. (a) Classical single channel transition interfacing an array of power amplifiers with a substrate integrated waveguide (SIW); (b) The novel transition where an array of PAs is interfaced to an SIW via multiple spatially distributed and strongly coupled microstrip lines (MLs). Also visualized is the transfer from the ML mode(s) to the fundamental TE₁₀ SIW mode. The MLs are closely spaced and, hence, strongly coupled, which causes mutual coupling effects to play a critical role in the proposed transition performance and its design. ©2018, IEEE. Reprinted, with permission, from [40, Fig. 1].

such a network occupies space and increases power losses, especially at mm-wave frequencies. To overcome these limitations in the above designs, active load modulation has been achieved through the mutual coupling between two spatially-separated identical antennas [52], [53] or two symmetrically located feeding points of a single antenna [54] [compare Fig. 5(a) and Fig. 5(b)]. The resulting antennas were therefore simultaneously acting as a radiating element and a Doherty power combiner, thereby for the first time demonstrating on-antenna power combining for DPAs. A common disadvantage of these designs, however, is that intermediate impedance matching circuitry at one of the PA branches is required, which increases its size and losses. Most importantly, this approach does not guarantee optimum performance, since the optimal loading condition for DPAs is highly non-symmetric [55], and therefore the Doherty antenna impedance matrix must be non-symmetric as well, if no extra impedance matching circuitry

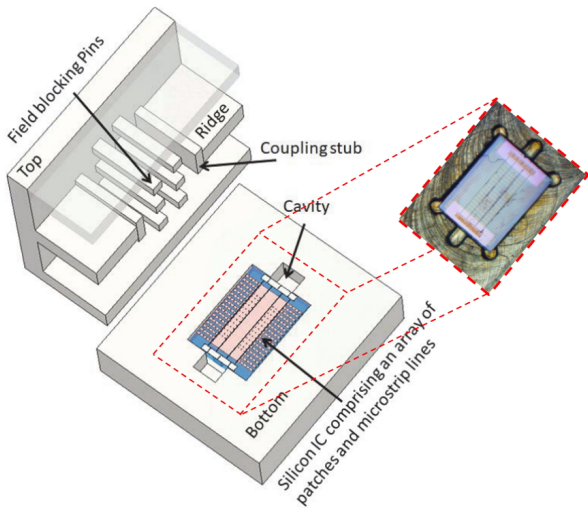


Fig. 4. Back-to-back E-band contactless IC-to-waveguide transition. The ridge waveguide field excites a metal cavity where four probes in the BEOL of the Silicon IC couple the resonant cavity field onto the four on-chip microstrip lines [41].

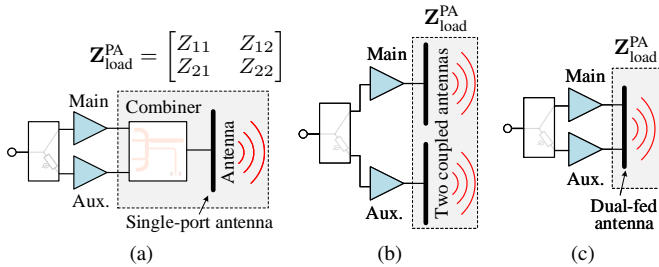


Fig. 5. Doherty PA-Antenna integration approaches: (a) conventional approach, where the main- and the auxiliary PAs are connected to the antenna via a tailored combiner network; (b) integration approach employing on-antenna power combining with two spatially-separated antenna elements; and (c) the proposed approach in [51] where a dual-fed antenna with non-symmetrical feeding enables on-antenna power combining and on-antenna matching directly to the optimal PA impedances.

is to be added.

An improved integrated antenna-integrated DPA concept has been proposed in [51], where the above problems are solved by synthesizing a dual-fed antenna with a non-symmetrical impedance matrix that is directly connected to the branches of the DPA and provides the optimal non-symmetrical impedance matrix for high-efficiency DPA operation. This integration approach allows to simultaneously eliminate intermediate power-combining and impedance-transforming networks by employing on-antenna power combining and on-antenna matching directly to the optimal PA impedances [cf. Fig. 5(c)].

The key design implementation challenges of such a highly integrated antenna-DPA system are: (i) to satisfy the optimal impedance matching condition and desired power-combining requirement over a relatively wide frequency band, and a required scan range when used in arrays of such antenna elements; (ii) to reduce the antenna radiation pattern variation as a function of input power due to the different non-linear

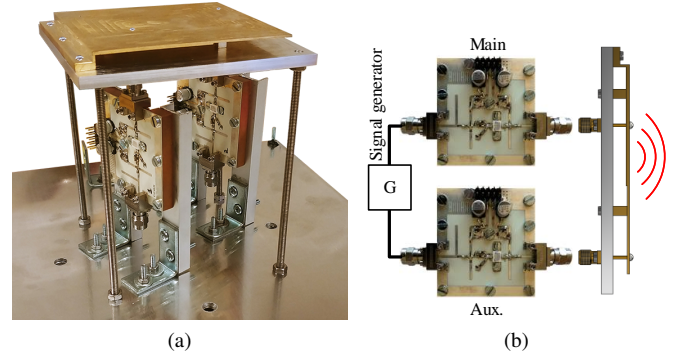


Fig. 6. The antenna and PA-testboard for the Doherty PA-Antenna integration approach in Fig. 5(c) [51]. The antenna is a dual-fed PIFA element with non-symmetrical impedance matrix, operating at 2.14GHz. The PA test boards are made modular by including SMA-connectors; this allows for characterization of the PA test boards in Doherty configuration using either the antenna combiner (Fig. 5(c)) or a conventional circuit combiner (Fig. 5(a)). A dual-channel signal generator is used to excite the PAs with a given amplitude and phase difference. The SMA connectors would not be included in a final integrated design.

TABLE II

SUMMARY OF THE OTA CHARACTERIZATION OF THE INTEGRATED DOHERTY PA-ANTENNA SYSTEM IN FIG. 6: MAXIMUM OUTPUT POWER P_{MAX} AND DRAIN EFFICIENCY η WITH APPROXIMATED MEASUREMENT UNCERTAINTY AND CORRESPONDING TRUST REGION OF THE EFFICIENCY.

	P_{max} , [dB]	$\eta @ P_{max}$, [%]	$\eta @ -6$ dB OPBO, [%]	P_{max} uncertainty, [dB]	η trust region @ P_{max} , [%]
sim.	44	64	62	–	–
AC	44	64	56	± 1.3	48...86
RC	33.5	63	59	± 0.35	58...68

output currents versus input power of the main and auxiliary PAs, and; (iii) to improve the accuracy of the measured output power and efficiency due to different sources of measurement uncertainties (i.e. the above mentioned variations of the antenna pattern shape, and possible degradation of the antenna-PA impedance match condition for certain measurement scenarios and methods).

D. OTA characterization methods

The above mentioned challenge on the measurement accuracy involves the research on the Over-The-Air (OTA) characterization. Relevant questions are: Which OTA methods and chambers are suitable for integrated antenna systems, where individual antenna element ports are either not accessible or not available? How to control and possibility mitigate the measurement uncertainties as introduced by the different transmitted signals of the PAs, and the corresponding variations of the antenna impedance and radiation characteristics in the measurement process? In [51], an OTA-characterization method in a reverberation chamber (RC) has been introduced to assess the efficiency of the integrated DPA antenna system shown in Fig. 6. This method has seen to yield the measurement accuracies in the order of ± 0.35 dB in terms of the transmitter efficiency (cf. Table II). At the same time, the measurements in an anechoic chamber (AC) with the same system has shown

to suffer from relatively larger measurement uncertainties (in the order of ± 1.3 dB) and therefore require a complex and time-consuming calibration procedure to correct for the above mentioned varying antenna characteristics.

IV. CONCLUSION

The latest studies highlighting some of the key results and lessons in the research area of circuit-antenna co-integration solutions for active beamforming receiving and transmitting array antennas have been presented. The directions of future studies reflect the trend towards stronger integration between multiple components and sub-systems, where the focus is on more sophisticated multi-amplifier architectures and multi-functional antenna element designs for optimum overall system performance, and reduced cost. For such systems, it is of importance to investigate wide-band solutions and include the array mutual coupling effects in the course of the antenna-amplifier co-design process. Finally, improving the Over-The-Air characterization methods, or developing new ones, that take into account measurement uncertainties which are specific for such integrated active antenna systems is of high demand as well.

ACKNOWLEDGMENT

This overview paper is based on the research which has been carried out in collaboration between the author and her-collaborators at different research organizations, including The Netherlands Institute for Radio Astronomy ASTRON, Chalmers University of Technology, Brigham Young University (USA), Stellenbosch University (South Africa), Technical University of Eindhoven (The Netherlands), as well as industrial partners, including Ericsson AB (Sweden), SAAB AB (Sweden), RUAG AB (Sweden), Keysight Technologies (Belgium), Gapwaves AB (Sweden), Bluetest AB (Sweden), and NXP Semiconductors (The Netherlands). Special acknowledgement goes (in no particular order) to A. van Ardenne, J.G. Bij de Vaate, Wim van Cappellen, B. Woestenburger, K.W. Warnick, late P.S. Kildal, D. B. Davidson, P. Meyer, D. Prinsloo, P. D. Patel, S. Wijnholds, R. Maaskant, O. Iupikov, M. Arts, W.-C. Liao, A. Roey, A. Aljarosha, T. Emanuelsson, V. Vassilev, M. Johansson, A. Hook, J. Wettergren, M. Dieudonne, H. Frid, J. Van Hese, E. Pucci, B. Goransson, A. B. Wikstrom, J. Johansson, B. Berglund, P. Ingvarson, P. Persson, P. Magnusson, S. Agneessens, W. Hallberg, A. Uz. Zaman, K. Buisman, P. Olanders, U. Gustavsson, D. Akesson, T. Eriksson, M. Geurts, C. Fager, R. Rehammar, A. B. Smolders, M. Matters-Krammerer, and U. Johannsen. Special acknowledgment to the funding agencies: Antenna Competence Research Centre CHASE-ON Centre Project 'Integrated Antenna Arrays' financed by the Swedish government Agency of Innovation Systems (VINNOVA), Chalmers University of Technology, Royal Institute of Technology (Stockholm), Ericsson, Saab, Ruag Space, Keysight Technologies, and Gapwaves; INITIATE project, financed by the strategic innovation program Smarter Electronic Systems, a joint effort by VINNOVA,

Formas, and the Swedish Energy Agency; the Silicon-based Ka-band massive MIMO antenna systems for new telecommunication services (SILIKA) project, funded by the European Unions Horizon 2020 research and innovation program under the Marie Sklodowska Curie grant agreement #721732; The Netherlands Organization for Scientific Research, NWO VIDI project, grant no. 14852 where M. Ivashina is part of the user committee. Furthermore, the author is thankful to B. Veidt and L. Belostotski for providing high-quality photos for Fig.1.

REFERENCES

- [1] B. L. G. Jonsson, C. I. Kolitsidas, and N. Hussain, "Array antenna limitations," *IEEE Antennas Wireless Propag. Lett.*, vol. 12, pp. 1539–1542, 2013.
- [2] K. F. Warnick, R. Maaskant, M. V. Ivashina, D. B. Davidson, and B. D. Jeffs, *Phased Arrays for Radio Astronomy, Remote Sensing, and Satellite Communications*. Cambridge: Cambridge University Press, 2018.
- [3] K. Hausmair, P. N. Landin, U. Gustavsson, C. Fager, and T. Eriksson, "Digital predistortion for multi-antenna transmitters affected by antenna crosstalk," *IEEE Trans. Microw. Theory Tech.*, vol. 66, no. 3, pp. 1524–1535, March 2018.
- [4] J. Huang, "L-band phased array antennas for mobile satellite communications," in *37th IEEE Vehicular Technology Conf.*, vol. 37, June 1987, pp. 113–117.
- [5] M. Geissler, F. Woetzel, M. Bottcher, S. Korthoff, A. Lauer, M. Eube, and R. Gieron, "Innovative phased array antenna for maritime satellite communications," in *2009 3rd European Conf. on Antennas and Propagation*, March 2009, pp. 735–739.
- [6] B. Tomasic, J. Turtle, R. Schmier, S. Bharj, and P. Oleski, "The geodesic dome phased array antenna for satellite control and communication - subarray design, development and demonstration," in *IEEE Int. Symp. on Phased Array Systems and Technology*, 2003., Oct 2003, pp. 411–416.
- [7] The SMOS website. [Online]. Available: https://en.wikipedia.org/wiki/Soil_Moisture_and_Ocean_Salinity
- [8] O. A. Iupikov, M. V. Ivashina, N. Skou, C. Cappellin, K. Pontoppidan, and C. G. M. van 't Klooster, "Multibeam focal plane arrays with digital beamforming for high precision space-borne ocean remote sensing," *IEEE Trans. Antennas Propag.*, vol. 66, no. 2, pp. 737–748, Feb 2018.
- [9] G. W. Kant, P. D. Patel, S. J. Wijnholds, M. Ruiter, and E. van der Wal, "EMBRACE: A multi-beam 20,000-element radio astronomical phased array antenna demonstrator," *IEEE Trans. Antennas Propag.*, vol. 59, no. 6, pp. 1990–2003, June 2011.
- [10] S. Ellingson, T. Clarke, A. Cohen, J. Craig, N. Kassim, Y. Pihlstrom, L. Rickard, and G. Taylor, "The long wavelength array," *IEEE Trans. Antennas Propag.*, vol. 97, no. 8, pp. 1421–1430, Aug. 2009.
- [11] S. Hay and T. Bird, *Applications of Phased Array Feeders in Reflector Antennas*, Z. Chen, D. Liu, H. Nakano, X. Quing, and T. Zwick, Eds. Springer, Singapore, Oct 2016.
- [12] E. E. M. Woestenburger, "Noise matching in dense phased arrays," Netherlands Institute for Radio Astronomy, Dwingeloo, The Netherlands, Tech. Rep. Tech. Rep. RP-083, 2005.
- [13] R. Maaskant and B. Woestenburger, "Applying the active antenna impedance to achieve noise match in receiving array antennas," in *Proc. IEEE AP-S International Symposium*, Honolulu, Hawaii, Jun. 2007, pp. 5889–5892.
- [14] E. E. M. Woestenburger, L. Bakker, and M. V. Ivashina, "Experimental results for the sensitivity of a low noise aperture array tile for the SKA," *IEEE Trans. Antennas Propag.*, vol. 60, no. 2, pp. 915–921, Feb 2012.
- [15] J. P. Weem and Z. Popovic, "A method for determining noise coupling in a phased array antenna," in *Microwave Symp. Digest. (IEEE MTT-S)*, Phoenix, Arizona, May 2001, pp. 271–274.
- [16] R. Sarkis, B. Veidt, and C. Craeye, "Fast numerical method for focal plane array simulation of 3D Vivaldi antennas," in *2012 Int. Conf. on Electromagnetics in Advanced Applications*, Sep. 2012, pp. 772–775.
- [17] K. F. Warnick and M. A. Jensen, "Effects of mutual coupling on interference mitigation with a focal plane array," *IEEE Trans. Antennas Propag.*, vol. 53, no. 8, pp. 2490–2498, Aug. 2005.

- [18] R. Maaskant, E. E. M. Woestenburger, and M. J. Arts, "A generalized method of modeling the sensitivity of array antennas at system level," in *Proc. 34th European Microwave Conf.*, Amsterdam, Oct. 2004, pp. 1541–1544.
- [19] M. V. Ivashina, O. Iupikov, R. Maaskant, W. A. van Cappellen, and T. Oosterloo, "An optimal beamforming strategy for wide-field surveys with phased-array-fed reflector antennas," *IEEE Trans. Antennas Propag.*, vol. 59, no. 6, pp. 1864–1875, Jun. 2011.
- [20] K. F. Warnick and B. D. Jeffs, "Efficiencies and system temperature for a beamforming array," *IEEE Antennas Wireless Propag. Lett.*, vol. 7, no. 1, pp. 565–568, 2008.
- [21] M. V. Ivashina, R. Maaskant, and B. Woestenburger, "Equivalent system representation to model the beam sensitivity of receiving antenna arrays," *IEEE Antennas Wireless Propag. Lett.*, vol. 7, no. 1, pp. 733–737, Jan. 2008.
- [22] D. S. Prinsloo, R. Maaskant, M. V. Ivashina, and P. Meyer, "Mixed-mode sensitivity analysis of a combined differential and common mode active receiving antenna providing near-hemispherical field-of-view coverage," *IEEE Trans. Antennas Propag.*, vol. 62, no. 8, pp. 3951–3961, Aug 2014.
- [23] K. F. Warnick, M. V. Ivashina, R. Maaskant, and E. E. M. Woestenburger, "Unified definitions of efficiencies and system noise temperature for receiving antenna arrays," *IEEE Trans. Antennas Propag.*, vol. 58, no. 6, pp. 2121–2125, Jan. 2010.
- [24] "IEEE Standard for Definitions of Terms for Antennas," *IEEE Std 145-2013 (Revision of IEEE Std 145-1993)*, pp. 1–50, March 2014.
- [25] K. F. Warnick, D. Carter, T. Webb, J. Landon, M. Elmer, and B. D. Jeffs, "Design and characterization of an active impedance matched low-noise phased array feed," *IEEE Trans. Antennas Propag.*, vol. 59, no. 6, pp. 1876–1885, June 2011.
- [26] R. D. Shaw, S. G. Hay, and Y. Ranga, "Development of a low-noise active balun for a dual-polarized planar connected array antenna for ASKAP," in *2012 Int. Conf. on Electromagnetics in Advanced Applications*, Sep. 2012, pp. 438–441.
- [27] M. Arts, M. Ivashina, O. Iupikov, L. Bakker, and R. van den Brink, "Design of a low-loss low-noise tapered slot phased array feed for reflector antennas," in *Proc. European Conference on Antennas and Propag. (EuCAP)*, Barcelona, Spain, Apr. 2010, pp. 1–5.
- [28] A. J. Beaulieu, L. Belostotski, T. Burgess, B. Veidt, and J. W. Haslett, "Noise performance of a phased-array feed with CMOS low-noise amplifiers," *IEEE Antennas Wireless Propag. Lett.*, vol. 15, pp. 1719–1722, 2016.
- [29] L. Belostotski, B. Veidt, K. F. Warnick, and A. Madanayake, "Low-noise amplifier design considerations for use in antenna arrays," *IEEE Trans. Antennas Propag.*, vol. 63, no. 6, pp. 2508–2520, June 2015.
- [30] F. Rusek, D. Persson, B. K. Lau, E. G. Larsson, T. L. Marzetta, O. Edfors, and F. Tufvesson, "Scaling up MIMO: Opportunities and challenges with very large arrays," *IEEE Signal Process. Mag.*, vol. 30, no. 1, pp. 40–60, Jan. 2013.
- [31] Ericsson, RUAG, SAAB, and Keysight, "Emerging Applications and Systems Employing mm-Wave Frequency Integrated Antenna Arrays," Ericsson, RUAG, SAAB, Keysight, Tech. Rep., 2017.
- [32] W. Liao, R. Maaskant, T. Emanuelsson, M. Johansson, A. Höök, J. Wettergren, M. Dieudonne, and M. Ivashina, "A Ka-band active integrated antenna for 5G applications: Initial design flow," in *2018 2nd URSI Atlantic Radio Science Meeting (AT-RASC)*, Gran Canaria, Spain, May 2018, pp. 1–4.
- [33] S. Gupta, P. K. Nath, A. Agarwal, and B. K. Sarkar, "Integrated active antennas," *IETE Technical Review*, vol. 18, no. 2-3, pp. 139–146, 2001.
- [34] K. Chang, R. A. York, P. S. Hall, and T. Itoh, "Active integrated antennas," *IEICE Trans. Commun.*, vol. 50, no. 3, pp. 937–944, 2002.
- [35] W.-C. Liao, R. Maaskant, T. Emanuelsson, V. Vassilev, and M. Ivashina, "A K-band Directly Matched PA-Integrated Antenna for Efficient mm-Wave High-Power Generation," for submission to the *IEEE AWPL Lett., Special Cluster on "Antenna-in-Package, Antenna-on-Chip, Antenna-IC Interface: Joint Design and Co-integration"*, 2019.
- [36] B. Goettel, P. Pahl, C. Kutschker, S. Malz, U. R. Pfeiffer, and T. Zwick, "Active multiple feed on-chip antennas with efficient in-antenna power combining operating at 200–320 GHz," *IEEE Trans. Antennas Propag.*, vol. 65, no. 2, pp. 416–423, Feb 2017.
- [37] K. C. Gupta and P. S. Hall, Eds., *Analysis and Design of Integrated Circuit-Antenna Modules*. Wiley, 1999.
- [38] M. P. DeLisio and R. A. York, "Quasi-optical and spatial power combining," *IEEE Trans. Microw. Theory Tech.*, vol. 50, no. 3, pp. 929–936, Mar. 2002.
- [39] T. Chi, S. Li, J. S. Park, and H. Wang, "A multifeed antenna for high-efficiency on-antenna power combining," *IEEE Trans. Antennas Propag.*, vol. 65, no. 12, pp. 6937–6951, Dec. 2017.
- [40] A. Roev, R. Maaskant, A. Höök, and M. Ivashina, "Wideband mm-wave transition between a coupled microstrip line array and siw for high-power generation mmics," *IEEE Microw. Wireless Compon. Lett.*, vol. 28, no. 10, pp. 867–869, Oct 2018.
- [41] P. Kaul, A. Aljarosha, A. B. Smolders, P. Baltus, M. Matters-Kammerer, and R. Maaskant, "An E-band silicon-IC-to-waveguide contactless transition incorporating a low-loss spatial power combiner," in *2018 Asia-Pacific Microwave Conf. (APMC)*, Nov 2018, pp. 1528–1530.
- [42] B. Goettel, J. Schäfer, A. Bhutani, H. Gulan, and T. Zwick, "In-antenna power-combining methods," in *2017 11th European Conf. on Antennas and Propagation (EUCAP)*, March 2017, pp. 2776–2730.
- [43] K. Sengupta and A. Hajimiri, "THz signal generation, radiation, and beamforming in silicon: a circuit and electromagnetics co-design approach," in *RF and mm-Wave Power Generation in Silicon*, H. Wang and K. Sengupta, Eds. Elsevier Inc., 2016, pp. 485–518.
- [44] R. Maaskant, O. Iupikov, C. A. H. M. van Puijenbroek, W. Liao, M. Matters-Kammerer, and M. Ivashina, "Deep integration antenna array: Design philosophy and principles," in *European Conf. on Antennas and Propagation (EuCAP2019)*, April 2019, pp. 1–5.
- [45] K. Datta and H. Hashemi, "2.9 A 29 dBm 18.5% peak PAE mm-wave digital power amplifier with dynamic load modulation," in *2015 IEEE Int. Solid-State Circuits Conf. - (ISSCC) Digest of Technical Papers*, Feb. 2015, pp. 1–3.
- [46] F. Golcuk, O. D. Gurbuz, and G. M. Rebeiz, "A 0.39–0.44 THz 2x4 amplifier-quadrupler array with peak EIRP of 34 dBm," *IEEE Trans. Microw. Theory Tech.*, vol. 61, no. 12, pp. 4483–4491, Dec. 2013.
- [47] N. Hasegawa and N. Shinohara, "C-band active-antenna design for effective integration with a GaN amplifier," *IEEE Trans. Microw. Theory Tech.*, vol. 65, no. 12, pp. 4976–4983, Dec. 2017.
- [48] F. H. Raab, P. Asbeck, S. Cripps, P. B. Kenington, Z. B. Popovic, N. Potheary, J. F. Sevic, and N. O. Sokal, "Power amplifiers and transmitters for RF and microwave," *IEEE Trans. Microw. Theory Tech.*, vol. 50, no. 3, pp. 814–826, Mar. 2002.
- [49] F. P. van der Wilt, E. Habekott, and A. B. Smolders, "A non-isolated power-combining antenna for outphasing radio transmitters," *IEEE Trans. Antennas Propag.*, vol. 64, no. 2, pp. 761–766, Feb 2016.
- [50] S. Li, T. Chi, H. T. Nguyen, T. Huang, and H. Wang, "A 28 GHz Packaged Chireix Transmitter with Direct on-Antenna Outphasing Load Modulation Achieving 56%/38% PA Efficiency at Peak/6dB Back-Off Output Power," in *2018 IEEE Radio Frequency Integrated Circuits Symp. (RFIC)*, June 2018, pp. 68–71.
- [51] O. Iupikov, W. Hallberg, R. Maaskant, C. Fager, R. Rehammar, and M. Ivashina, "A Dual-Fed PIFA Antenna Element with Non-Symmetric Impedance Matrix for High-Efficiency Doherty Transmitters: Integrated Design and OTA-characterization," submitted to the *IEEE Trans. Antennas Propag.*
- [52] S. Jia, W. Chen, and D. Schreurs, "A novel Doherty transmitter based on antenna active load modulation," *IEEE Microw. Wireless Compon. Lett.*, vol. 25, no. 4, pp. 271–273, Apr. 2015.
- [53] Y. Zhao, F. M. Ghannouchi, M. Helaoui, X. Li, X. Du, W. Zhang, and T. Apperley, "Doherty transmitter based on monopole array antenna active load modulation," *IEEE Microw. Wireless Compon. Lett.*, vol. 28, no. 10, pp. 927–929, Oct. 2018.
- [54] H. T. Nguyen, T. Chi, S. Li, and H. Wang, "A linear high-efficiency millimeter-wave CMOS Doherty radiator leveraging multi-feed on-antenna active load modulation," *IEEE J. Solid-State Circuits*, vol. 53, no. 12, pp. 3587–3598, Dec. 2018.
- [55] M. Özen, K. Andersson, and C. Fager, "Symmetrical Doherty power amplifier with extended efficiency range," *IEEE Trans. Microw. Theory Tech.*, vol. 64, no. 4, pp. 1273–1284, Apr. 2016.